reproductive medicine

MDPI

Article

Adaptations in the Hippocampus during the Fetal to Neonatal Transition in Guinea Pigs

Julia C. Shaw [1,2,*], Rebecca M. Dyson [3,4], Hannah K. Palliser [1,2], Gabrielle K. Crombie [1,2], Mary J. Berry [3,4] and Jonathan J. Hirst [1,2]

1 School of Biomedical Sciences and Pharmacy, University of Newcastle, Callaghan 2308, Australia; hannah.palliser@newcastle.edu.au (H.K.P.); gabrielle.crombie@uon.edu.au (G.K.C.); jon.hirst@newcastle.edu.au (J.J.H.)
2 Mothers and Babies Research Centre, Hunter Medical Research Institute, New Lambton Heights 2305, Australia
3 Department of Paediatrics and Child Health, University of Otago, Wellington 6021, New Zealand; becs.dyson@otago.ac.nz (R.M.D.); max.berry@otago.ac.nz (M.J.B.)
4 Centre for Translational Physiology, University of Otago, Wellington 6021, New Zealand
* Correspondence: julia.c.shaw@newcastle.edu.au; Tel.: +61-4042-0485

Abstract: (Background) The transition from in utero to ex utero life is associated with rapid changes in the brain that are both protective and required for newborn functional activities, allowing adaption to the changing environment. The current study aimed to reveal new insights into adaptations required for normal ongoing brain development and function after birth. (Methods) Time-mated dams were randomly allocated to fetal collection at gestational age 68 or spontaneous term delivery followed by neonatal collection within 24 h of birth. Immunohistochemistry was performed to examine mature myelin formation and neuronal nuclei coverage. RT-PCR was used to quantify the mRNA expression of key markers of the oligodendrocyte lineage, neuronal development, and GABAergic/glutamatergic pathway maturation. (Results) Mature myelin was reduced in the subcortical white matter of the neonate, whilst neuronal nuclei coverage was increased in both the hippocampus and the overlying cortical region. Increased mRNA expression in neonates was observed for oligodendrocyte and neuronal markers. There were also widespread mRNA changes across the inhibitory GABAergic and excitatory glutamatergic pathways in neonates. (Conclusions) This study has identified important adaptations in the expression of key neurodevelopmental structures, including oligodendrocytes and neurons, that may be essential for appropriate transition in neurodevelopment to the postnatal period.

Keywords: neurodevelopment; birth transition; hippocampus

Citation: Shaw, J.C.; Dyson, R.M.; Palliser, H.K.; Crombie, G.K.; Berry, M.J.; Hirst, J.J. Adaptations in the Hippocampus during the Fetal to Neonatal Transition in Guinea Pigs. *Reprod. Med.* **2022**, *3*, 85–100. https://doi.org/10.3390/reprodmed3020008

Academic Editor: Ilona Hromadnikova

Received: 29 March 2022
Accepted: 13 April 2022
Published: 18 April 2022

1. Introduction

Fetal to neonatal transition is a period of rapid physiological and functional change, affecting organs ranging from the heart and the lungs to the brain. The separation of the fetus from the in utero environment is also associated with a reduction in placentally-derived neurotrophic and neuroprotective support [1]. The neurosteroid, allopregnanolone, is particularly important during this transition by controlling excitability in the late gestation CNS of long gestation species. During fetal life placentally derived support for allopregnanolone synthesis maintains tonic inhibition and the fetal 'sleep-like' state that is seen in late gestation [2]. This is mediated by inhibitory action of allopregnanolone on extra-synaptic $GABA_A$ receptors throughout the fetal brain [3]. A reduction in this tonic inhibition, as shown in fetal sheep following infusion of the allopregnanolone synthesis inhibitor finasteride, is associated with increased electrocortical activity, damaging seizures, and cell death [4,5]. Thus, early, or inappropriate removal from the inhibitory in utero environment can be rather damaging and expose the developing brain to excitotoxicity. Indeed, exogenous neurosteroid analogues have been trialled for reducing seizures in

neonatal sheep and preterm guinea pigs [6–8]. These findings raise the question of what key changes occur in the neonatal brain that allow it to cope with the loss of the inhibitory environment and the subsequent exposure to a stimulating ex utero environment.

Insights into the key changes that are integral to correct neurodevelopment can be obtained from studies focused on perinatal compromises in late gestation, such as preterm birth, and in particular exposure to hypoxia at birth. In previous studies, we and others have shown that a major cell type vulnerable to late gestation prenatal stress and preterm birth is oligodendrocytes [9–12]. Oligodendrocytes develop in a lineage that is sensitive to damage. This involves progenitor cells developing into preoligodendrocyte cells then to mature oligodendrocytes capable of producing myelin [13,14]. The production of myelin and myelination of axons begins ~30 weeks in the human, with late gestation representing a period of intense myelination throughout the fetal brain [13,15]. Magnetic resonance and fractional anisotropy imaging from neonates born very preterm show a clear lack of myelination compared to those born at term, even at corrected ages [16,17], but subtle reductions in late preterm infants are more difficult to identify. In our guinea pig model of preterm birth, we have identified reduced oligodendrocyte lineage cells at all developmental stages, in brain regions such as the cerebellum, hippocampus and cortex [9–11,18]. Furthermore, there is a long-term reduction in myelin formation in these animals which is associated with hyperactive behavior in males, and anxious behavior in females [9]. This highlights that early exposure to the ex utero environment results in a dysregulation in ongoing neurodevelopmental processes, suggesting that key transitional changes have not occurred. Hypoxia at birth represents a major challenge for the newborn with rapidly falling levels of allopregnanolone, and therefore inhibitory tone, creating vulnerability to excitotoxicity [5,19]. In early preterm delivery, these processes adversely affect neuronal survival leading to marked cell loss which may involve loss of trophic support. As gestation progresses, cells of the oligodendrocyte lineage rapidly develop, and the lineage becomes increasingly more susceptible to a combination of a loss of direct trophic support and great excitation [20,21].

Together, the above studies indicate that specific changes in major neural cell types including oligodendrocytes and neurons are required for optimal transition to the ex utero environment in order to resist the effects of the greater excitatory environment. It is important to understand these protective changes in order to develop approaches to sufficiently mitigate these processes following preterm birth. In the current study we have compared the hippocampus of the near-term fetus with the 24-h old neonate. We proposed that key changes in major excitatory and inhibitory pathways are initiated in the fetal to neonatal transition and that these changes compensate for the loss of placental support for brain development. This study was performed using the developmentally relevant guinea pig, which is a relatively long gestation species that delivers precocial young with similar brain development timelines to the human [22]. We have focused on transitional effects on oligodendrocytes and neurons, in addition to markers in key pathways known to control inhibition (GABAergic) and excitation (glutamatergic), and neurosteroid synthesis.

2. Materials and Methods

Unless specified otherwise, all reagents were supplied by Sigma Aldrich (Castle Hill, NSW, Australia).

2.1. Animals

Mature breeding Dunkin Hartley female guinea pigs were obtained from the University of Otago Wellington Biomedical Research Unit. Guinea pigs were housed indoors under a 12 h light/dark cycle and supplied with standard guinea pig pellets, (Specialty Feeds, Glen Forrest, WA, Australia), hay, fresh vegetables, and drinking water supplemented with Vitamin C. Pregnant dams were randomly allocated to either near term fetal collection at gestational age 68 (GA68; n = 14 dams) or spontaneous term (n = 10 dams) delivery. No more than 2 fetuses or pups/sex per dam were used in the study, with pup numbers per

group displayed in the results section. The same animals were used for protein and mRNA analyses. Term delivery in this cohort is generally GA69 [23]. Term delivery dams received no further intervention, with pups delivered spontaneously and tissue collection occurring within 24 h of delivery (postnatal day 1; PND1). Fetuses (GA68) were collected from dams whilst the dam was under isoflurane with euthanasia occurring within the amniotic sac and prior to separation from the placenta. Neonates were euthanized by exsanguination under isoflurane. Body measurements and organ weights were taken (see results section), including subcutaneous (back of the neck fat pad) and visceral (surrounding kidneys) fat which was excised and weighed. Each brain was then sectioned in the sagittal plane to separate the hemispheres with the left hemisphere fixed in 4% paraformaldehyde, and the right hemisphere further dissected and frozen in liquid nitrogen.

2.2. Immunohistochemistry

Immunohistochemistry was performed on 8 µm sections of paraffin-embedded brains cut using a Leica RM2145 Microtome (Leica Microsystems Pty Ltd., North Ryde, NSW, Australia) to quantify mature myelinating oligodendrocyte and neuronal nuclei expression in the CA1 region of the dorsal hippocampus and overlying subcortical white matter. Serial washes in xylene and ethanol dewaxed and rehydrated the tissue sections. Antigen retrieval was performed by incubation in citrate buffer (pH 6.0) at 90–95 °C (25 min, followed by cooling for 15 min). Prior to antibody incubation, endogenous peroxidase activity was blocked by incubation in 3% hydrogen peroxide in PBS (20 min) and non-specific staining by a goat serum block (2% goat serum, 0.4% BSA, 0.3% TritonX in PBS; 1 h). Tissue sections were then incubated overnight in primary antibodies at 1:1000 dilution (myelin basic protein [MBP] M9434; neuronal nuclei [NeuN] MAB377 Millipore [Burlington, MA, USA]), before secondary antibody incubation for 1 h at 1:300 dilution (biotinylated anti-rat IgG B7139; biotinylated anti-mouse IgG B6649). Streptavidin-biotin-horseradish complex (ab7403 Abcam [Cambridge, UK]) was then used for the tertiary incubation for 1 h at a 1:400 dilution. All incubations took place at room temperature unless specified. Incubation in 3,3′-diaminobenzidine tetrahydrochloride solution (Metal Enhanced DAB Substrate Kit; ThermoFisher Scientific, Scoresby, VIC, Australia) revealed immunolabelling.

Stained slides were digitally imaged using the Aperio imaging system (Leica Biosystems, North Ryde, NSW, Australia). Image analysis was then performed using a numbering system to ensure the group was blinded during the analysis. ImageJ v1.47 (National Institutes of Health, Bethesda, MD, USA) was used to calculate percent area coverage of positive staining by conversion to grayscale and then binary, and manually adjusting the threshold based on the original stained image. Overall average of staining was calculated by taking the average of four images captured from two consecutive sections per animal, i.e., a total of eight images/region/animal.

2.3. Real Time PCR

Frozen hippocampal tissue was prepared for PCR as previously described [9,10]. Prior to RNA extraction, the tissue was homogenised in RLT Plus Buffer (Qiagen RNeasy Plus Mini Kit, Qiagen Pty Ltd., Chadstone, VIC, Australia) using a Precellys 24 dual-tissue homogenizer (Bertin Technologies, Montigny-le-Bretonneux, France). The Qiagen RNeasy Plus Mini Kit (Qiagen) was then used to perform RNA extractions by following the manufacturer's instructions. The Superscript III Reverse Transcription Kit (Invitrogen, Waltham, MA, USA) was then used to synthesize cDNA on a GeneAmp 9700 PCR machine (Applied Biosystems, Life Technologies Pty Ltd., Mulgrave, NSW, Australia). The cDNA samples were then preamplified on the QuantStudio 6 Flex RT-PCR system (Applied Biosystems) using a PreAmp Master Mix (Fluidigm, San Francisco, CA, USA), according to the manufacturer's instructions. Relative mRNA expression analysis was conducted simultaneously on an integrated fluidic chip (Fluidigm). The primer master mix for each primer (0.5 pmole/µL, Fluidigm) and EVAGreen (Bio-Rad Laboratories, Hercules, CA, USA) was used to detect PCR products of the genes of interest (Table 1). RT-PCR was then

performed using the Biomark HD system (Fluidigm) and the results were analysed by RT-PCR analysis software v4.5.2 (Fluidigm), using the comparative CT method ($2^{\Delta\Delta Ct}$) of analysis with each sample normalised to four housekeeping genes (*ACTB*, *TBP*, *YWHAZ*, *UBE2D2*) and a calibrator. Means and SEM for genes not displayed in the results section can be found in the Supplementary Text.

Table 1. Guinea pig specific primers for high throughput Fluidigm mRNA quantification.

Gene ID	Protein	Forward Primer	Reverse Primer	Amplicon Size (bp)
ABAT	GABA aminotransferase (GABA-T)	GGATGTCCCAGCTTGTCACTA	TTGCTCCGGTACCACATGAA	85
ACTB	Beta actin (housekeeper)	TGCGTTACACCCTTTCTTGACA	ACAAAGCCATGCCAATCTCAT	72
AIF1	Allograft inflammatory factor 1	GGCTCTGGGGAGACATTCA	AGATCTCTTGCCCAGCATCA	60
BDNF	Brain derived neurotrophic factor	AATCGGCTGGCGGTTCATAA	AGCCACTATCTGCCCCTCTTA	75
CALB1	Calbindin	CTGACTGAGATGGCCAGGTTA	CCCACACATTTTAACTCCCTGAAA	75
CAPN1	Calpain1	TTCCCTCACTCTGAACGACAC	AGTGGAAGATGCCAGCGTAA	86
CAPN2	Calpain 2	TGCAGAAACTGATCCGAGTCC	TCCAGTTTGGGCAGTTGTCA	81
CAPNS1	Calpain small subunit 1	CGACACCCTGACCTGAAAAC	TGTGGTGTCGCTATCCATCA	81
CAST	Calpastatin	AAGCCAAGGAACCACTTCCA	AGGTATCTGGAGGACTGGAGAA	84
CKAP5	Cytoskeleton associated protein 5	AGGACATGTTGTGCCAACCA	GCCTCTTGCAGGGCTTGTA	75
CSPG4	Chondroitin sulfate proteoglycan 4 (NG2)	CTCCTCACCACCACCCTCAA	ACTCTTCAGCACAGCCCTCA	79
DLG4	Postsynaptic density protein 95 (PSD-95)	TATTCCCAGCACCTGGACAA	TCATGGCTGTGGGGTAATCA	70
DNMT1	DNA-methyltransferase 1	ACGACGTGGACCTCAAGTAC	CGAAGATGGACAGTGCCTCA	87
DNMT3A	DNA-methyltransferase 3A	GGGGACAAGAATGCCACCAA	CCAGCTCCCCAATGCCAAA	79
ENO2	Neuron specific enolase	TGACCTGACAGTGACCAACC	TTGACCTTGAGCAGCAGACA	81
FYN	Protein-tyrosine kinase	ACCGGTTACATTCCCAGCAA	GCGGCCAAGTTTTCCAAAGTA	81
GABRA1	$GABA_A$ receptor subunit alpha 1	CTCAAGCCCGCAATGAAGAAA	TCCAGTCAACGTGCTCAGAA	81
GABRA2	$GABA_A$ receptor subunit alpha 2	ACTAGGCCAATCAATTGGGAA	TCAAGTGGAAATGAGCTGTCA	80
GABRA3	$GABA_A$ receptor subunit alpha 3	TTGGCAGCTATGCCTACACA	ACCTCCACAGACTTGTTCTTCC	73
GABRA4	$GABA_A$ receptor subunit alpha 4	TGGACAAAGGGTCCTGAGAAA	CACTGTTTGCCCAATCAGATCA	84
GABRA5	$GABA_A$ receptor subunit alpha 5	TGGTTCATCGCTGTGTGCTA	CCCAGCCTCTCTTCGTGAAATA	85
GABRD	$GABA_A$ receptor subunit delta	ATGCTGGACCTGGAAAGCTA	GGATCTGCTCCTGGTTCTCA	76
GABRG2	$GABA_A$ receptor subunit gamma 2	AGGCAGATGCCCATTGGATA	TGTAGAGCACTCTGCCATCA	72
GAD1 (67)	Glutamate decarboxlase 1 (67 kDa)	AGCTCGCTACAAGTACTTCCC	TGTGTTCTGAGGTGAAGAGGAC	83
GAD2	Glutamate decarboxlase 2	GGCGCCATCTCCAACATGTA	TGCCCTTCTCCTTGACCTCA	73
GLS1	Glutaminase	CACGTTGGTCTTCCTGCAAA	GCACATCATGCCCATGACA	78
GRIA1	Glutamate ionotropic receptor AMPA 1 (GluA1)	TGAACGCAGGACTGTCAACA	AAGCTCGGTGTGATGAAGCA	72

Table 1. *Cont.*

Gene ID	Protein	Forward Primer	Reverse Primer	Amplicon Size (bp)
GRIA2	Glutamate ionotropic receptor AMPA 2 (GluA2)	GACACCTCACATCGACAACC	CGCCTCTTGAAAACTGGGAA	80
GRIA3	Glutamate ionotropic receptor AMPA 3 (GluA3)	CATGGCCAGGCAGAAGAAAA	ATGACCCAAAAGCCCCAGTA	76
GRIA4	Glutamate ionotropic receptor AMPA 4 (GluA4)	TGTCCTGGTGATGGCTGAAA	ATCCCCAGCATTTCCTCTCC	79
GRIN1	Glutamate ionotropic receptor 1 (GluN1)	AGAGCATCCACTTGAGCTTCC	TACACGCGCATCATCTCGAA	82
GRIN2A	Glutamate ionotropic receptor 2A (GluN2A)	TCGAGGATGCGAAGACACAA	AGCCTCGTCTTTGGAGCAATA	80
GRIN2B	Glutamate ionotropic receptor 2B (GluN2B)	GCACTAAGGAAGAAGCCACCTA	ATCCATGTGTAGCCGTAGCC	76
GRIN2C	Glutamate ionotropic receptor 2C (GluN2C)	ATGCACACCCACATGGTCAA	CGTCCAGCTTCCCCATCTTAA	79
GRIN2D	Glutamate ionotropic receptor 2D (GluN2D)	ACCTGGGATAACCGGGACTA	TGTCTCTGGTGAGGGAAATGAC	85
GRIN3A	Glutamate ionotropic receptor 3A (GluN3A)	AAGGGTTGCTGCCCTACAA	GCAAAAGTGGCAGGTCTCC	78
GRM1	Glutamate metabotropic receptor 1 (mGluR1)	GGGCAGACAGAGATGAAGTCA	CCTCTGGAGACTGCAGCTTTA	81
GRM2	Glutamate metabotropic receptor 2 (mGluR2)	GACTTCGTGCTCAACGTCAA	GCCATCTCCAAAACGGTCAA	87
GRM3	Glutamate metabotropic receptor 3 (mGluR3)	GCATACCCCAGGTGAGCTAC	TGCGCGCGAAGTAGTCATA	75
GRM4	Glutamate metabotropic receptor 4 (mGluR4)	ACGTCAAGAAGTGCACCAAC	AATCACGAACTGCACCTTCC	80
GRM5	Glutamate metabotropic receptor 5 (mGluR5)	AAGCTCCGGCCAGAAACAAA	CCTTCCAGCCGACACTGAAA	80
GRM7	Glutamate metabotropic receptor 7 (mGluR7)	GATCCTTGCAGCAGCCAAAA	TTTTGGATCCCCAGCTGTCA	77
GRM8	Glutamate metabotropic receptor 8 (mGluR8)	ACACTGGCTTCTGAGGGAAA	TGCAAACACCACCAATCTCC	82
HNRNPA2B1	Heterogeneous nuclear ribonucleoprotein A2/B1	TGGACCAGGACCAGGAAGTAA	CCCGTTATAGCCATCCCCAAA	82
IL1B	Interleukin 1 beta	ACGGCCCCAATAAGATGCA	TTTGCAGCTTGATCCCCTCA	75
INA	Alpha-internexin	ACAAGATCATCCGCACCAAC	GTGCACCTTTTCGATGAACAC	80
KIF1B	Kinesin family member 1B	AAGCATGACTCGGAGACCAA	GTTCACTTCCGGCTAGATCCA	76
MBP	Myelin basic protein	ACCTCCTCCGTCTCAAGGAAA	GCTCTGCCTCCATAGCCAAA	66
MOG	Myelin oligodendrocyte glycoprotein	GCAGCACAGACTGAGAGGAA	CCCTCAGAAAGTGGGGATCAA	77
NCAM1	Neural cell adhesion molecule 1	TTGTTCCCAGCCAAGGAGAA	TGTCTTTGGCATCTCCTGCTA	78
NEFH	Neurofilament heavy chain	CTCCGTATCGGCTTCACCAA	CCGTTGCTCAGCGTGTCTA	81
NEFL	Neurofilament light chain	TGATGCCCAGCTTGGAGAA	CTGCGTGCGGATCGATTTAA	77
NEFM	Neurofilament medium chain	GAGAGCAGCCTCGACTTCA	GGAGCGGGACAGCTTGTA	78
NFKB1	Nuclear factor kappa B subunit 1	AAGGCTCCCAATGCATCCAA	AATCTCCTCCCCGCCAGTTA	78
NR3C1	Glucocorticoid receptor	ACCACAGCCCCAAGTGAAAA	GGCCCAGTTTCTCCTGCTTAA	83
NR3C2	Mineralocorticoid receptor	GTGCCATTGTGAAAAGCCCTA	GCTGCAAACCGAAGATGTCA	86

Table 1. *Cont.*

Gene ID	Protein	Forward Primer	Reverse Primer	Amplicon Size (bp)
NTRK2	Neurotrophic receptor tyrosine kinase 2	CTCTAATGGGAGCAACACTCCA	GACAGGGATCTTGGTCATCCC	79
OLIG2	Oligodendrocyte transcription factor 2	GCACTCATCCTGGGGACAA	CCGACGACGTGGATGATGAA	78
PCBP1	Heterogeneous nuclear ribonucleoprotein E1	CTGGACGCCTACTCGATTCAA	TTGTCTTGCCACCTGGTTCA	78
PLP1	Proteolipid protein 1	TGCAGCAACATTGGTTTCCC	CTCGGCCCATGAGTTTAAGAAC	80
PVALB	Parvalbumin	AAGGATGGGGACGGCAAA	GGGTCCATCAGCTCTGCTTA	77
QKI	KH domain RNA binding	CTGCTGCAATAGTCCCTCCA	AGCTGGTGCCAACGTGTA	80
RBFOX3	RNA binding fox-1 homolog 3 (NeuN)	CACAGACAGACAGCCAACCA	CGGAAGGGGATGTTGGAGAC	88
SLC12A2	Sodium/potassium/chloride transporter	GGGGAAGAAAGTACTCCAACCA	ACACCCTTGATCCAGCCAAA	89
SLC12A5	Potassium-chloride cotransporter 2	CCTGTATGGCCACTGTGGTA	AGGATGACACAACCCAGGAA	79
SLC17A6	Vesicular glutamate transporter 2 (vGlut2)	TGCCATGCCTTTAGCTGGTA	CATGTACCAGACCATCCCAAAAC	91
SLC17A7	Vesicular glutamate transporter 1 (vGlut1)	CAGCCTTTTGCGGTTCCTAC	AACAGAGCTCCATCCCGAATAC	86
SLC17A8	Vesicular glutamate transporter 3 (vGlut3)	GGATGGGCTTCGGTCTTCTA	GCACTCATAGGCTTGCAACA	81
SLC1A2	Excitatory amino acid transporter 2 (EAAT2)	CACAGTCGTCTCCCTGTTGAA	CAGGCCCTTCTTGAGAACCA	76
SLC1A3	Excitatory amino acid transporter 1 (EAAT1)	TGACCAAAGGCAATGGGGAA	GCGGACTCCTTGCTGGAA	68
SLC32A1	Vesicular inhibitory amino acid transporter (vGAT)	ACACGACAAGCCCAAGATCA	TAGCACGAACATGCCCTGAA	76
SLC6A1	GABA transporter 1 (GAT1)	AGCGCTGCTTCTCCAACTAC	ATTGCGCTCCCAAAACTCCA	77
SLC6A11	GABA transporter 3 (GAT3)	ATCATGCTCTGCTGCCTGAA	CATAAGCCATGAAGCCCAAGAC	82
SRD5A1	Steroid 5 alpha-reductase 1	GGCTATGTTCGTCGTCCACTA	AAGGCTGACACACAGGTGAA	99
SRD5A2	Steroid 5 alpha-reductase 2	CGGCGAGATCACTGAATGGA	CTCCCGAGGAAACAAAGCGT	93
SST	Somatostatin	AAGCAGGAACTGGCCAAGTA	TGGGACAAATCTTCAGGTTCCA	92
STAR	Steroidogenic acute regulatory protein (StAR)	GGACCTTGAGAGGTTCCAGAA	AGCATTGTGCCCAGAAGGTA	74
SYP	Synaptophysin	TTCAGGCTGCACCAAGTGTA	GTAGTCCCCAACGAGGAAGAC	78
TBP	TATA-binding protein (housekeeper)	CAAGCGGTTTGCTGCTGTAA	CACCATCTTCCCGGAACTGAA	79
TSPO	Translocator protein	CCCATCTGGGGTACGCTGTA	AATCCACCCAGCTCCTTCCA	71
UBE2D2	Ubiquitin conjugating enzyme E2 D2 (housekeeper)	CAGTGCTGCGTGTTGTACATA	TGCTAGGAGGCAATGTTGGTA	76
VEGFA	Vascular endothelial growth factor A	GGAGAATGTCCCTCCCAGAA	GCCTCCCTAGAAGGGACAAA	84
YWHAZ	Tyrosine 3-monooxygenase (housekeeper)	GCTTCACAAGCAGAGAGCAA	CAGCAACTTCGGCCAAGTAA	76

Primer sequences for detection of genes of interest in the guinea pig hippocampus. Primer sequences are displayed from 5′3′ for forward and reverse primers.

2.4. Statistical Analyses

Data were analysed using Prism v9.0 (Graphpad Software Inc., La Jolla, CA, USA) and presented as mean ± SEM for each group with significance considered $p < 0.05$. To identify

differences between groups, the sexes were considered separately and comparisons between age were made by unpaired *t*-tests.

3. Results

3.1. Body and Organ Weights

At the time of tissue collection, body and absolute organ weights were recorded, and are displayed in Table 2. Within each sex, there was no significant difference in body, adrenal or subcutaneous fat weight. Female neonates had significantly lighter brains than fetuses ($p = 0.017$), but no significant difference for hippocampus or $\frac{1}{2}$ cerebellum weight. Conversely, there were no significant differences in brain or specific brain regions for males. Interestingly, liver and heart weights were significantly less for neonates of both sexes compared to fetuses (liver: males $p = 0.033$; females $p = 0.0095$; heart: males $p = 0.003$; females $p = 0.012$). Whilst there were no significant differences between neonate and fetal weight for kidneys or visceral fat for males, neonatal females had heavier kidneys than fetuses ($p = 0.046$) and less visceral fat ($p = 0.004$).

Table 2. Post-mortem body and absolute organ weights.

Sex	Delivery	N	Body Wgt	Brain Wgt	Hippo. Wgt	Cereb. Wgt	Liver Wgt	Heart Wgt	Kidney Wgt	Adren-als Wgt	Sub. Cut. Fat Wgt	Visc. Fat Wgt
Male	GA68 Fetus	7	102.0 ± 5.6	2.68 ± 0.03	0.114 ± 0.005	0.156 ± 0.010	5.32 ± 0.42	0.551 ± 0.026	0.742 ± 0.050	0.034 ± 0.004	1.57 ± 0.10	0.968 ± 0.066
	Term 24 h Neonate	8	97.2 ± 2.8	2.61 ± 0.05	0.112 ± 0.004	0.141 ± 0.005	3.97 ± 0.27 *	0.395 ± 0.018 *	0.834 ± 0.027	0.034 ± 0.002	1.40 ± 0.06	0.837 ± 0.037
Female	GA68 Fetus	7	96.4 ± 5.0	2.68 ± 0.04	0.128 ± 0.014	0.174 ± 0.013	5.35 ± 0.36	0.546 ± 0.047	0.725 ± 0.035	0.043 ± 0.005	1.33 ± 0.09	0.863 ± 0.031
	Term 24 h Neonate	7	98.6 ± 4.3	2.52 ± 0.04 *	0.123 ± 0.007	0.158 ± 0.010	3.91 ± 0.29 *	0.386 ± 0.024 *	0.849 ± 0.045 *	0.037 ± 0.005	1.22 ± 0.09	0.663 ± 0.050 *

Means and standard error of the means for body and organ weights recorded upon tissue collection. All weights are in grams. Wgt = weight, hippo = hippocampus, Cereb = cerebellum, Sub Cut = subcutaneous, Visc = visceral. Data presented as means ± SEM with * indicating significance at $p < 0.05$.

3.2. Myelination and Neuronal Nuclei Expression in the Hippocampus and Subcortical White Matter

Mature myelin and neuronal nuclei percent area coverage (Figure 1) was quantified by immunohistochemistry in the CA1 region of the hippocampus and overlying subcortical white matter. There was no significant difference in mature myelin coverage in the CA1 region of the hippocampus for either sex (Figure 1A,E), however there was a significant reduction in subcortical white matter myelination for term neonates compared to fetuses for both sexes (Figure 1B,E, males $p = 0.0005$ and females $p = 0.0043$). Conversely, area coverage for neuronal nuclei staining was significantly increased in the CA1 region of the hippocampus (Figure 1C,F) of neonates compared to fetuses for both males ($p = 0.0187$) and females ($p = 0.0032$). Additionally, neuronal nuclei area coverage was also significantly increased in the subcortical white matter (Figure 1D,F) of female neonates compared to fetuses ($p = 0.0165$), whilst there was no significant difference for males. Means and SEM are available in the Supplementary Text.

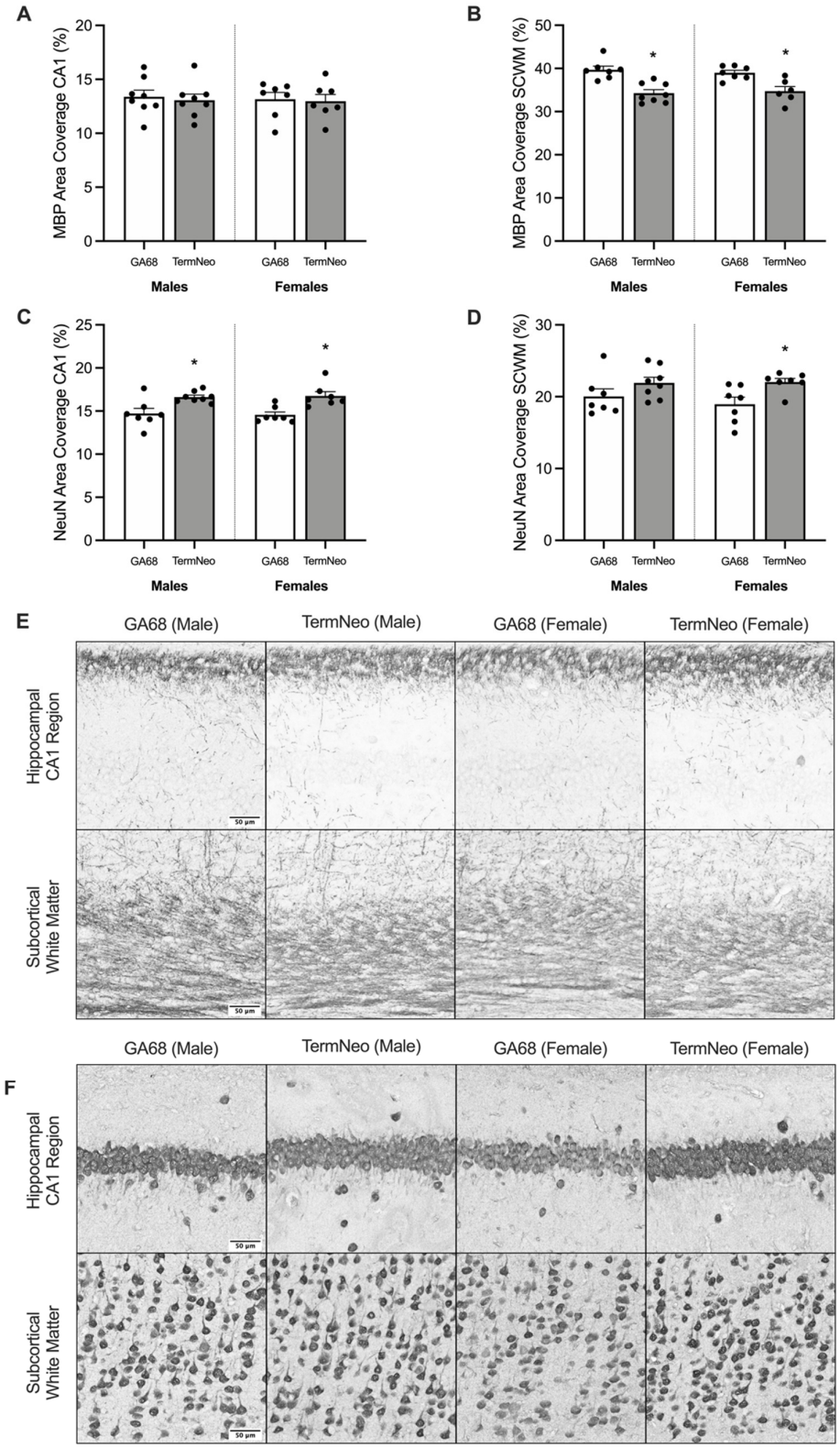

Figure 1. Myelin basic protein (MBP) and neuronal nuclei (NeuN) immunostaining was quantified in the brain of fetal GA68 (white; males $n = 7$, females $n = 7$) and term neonates (grey; males $n = 8$, females $n = 7$) for (**A**,**C**) the CA1 region of the hippocampus and (**B**,**D**) the overlying subcortical white matter. Data presented as means ± SEM with * indicating significance at $p < 0.05$. Representative photomicrographs of (**E**) MBP and (**F**) NeuN immunostaining of the CA1 region and overlying subcortical white matter. Scale bar = 50 µm.

3.3. Relative mRNA Expression of Oligodendrocyte Lineage and Neuron Markers

The relative mRNA expression of oligodendrocyte lineage markers, in addition to key genes involved in the production of myelin, were quantified in the hippocampus, and are displayed in Figure 2. As expected, the expression of *NCAM1* (oligodendrocyte precursor cells) was reduced in neonates, however, this only reached significance for the females (Figure 2A, males $p = 0.0713$; females $p = 0.0007$). Alternatively, expression of immature oligodendrocytes (*CSPG4*, Figure 2B) was significantly increased in neonates of both sexes compared to fetal levels (males $p = 0.0114$, females $p = 0.0039$), and expression of terminally myelinated oligodendrocytes (*MBP*, Figure 2C) was significantly increased in males ($p = 0.0154$) but did not reach significance females ($p = 0.0545$). Meanwhile, the expression of other mature oligodendrocyte markers (*PLP1*, Figure 2D; *MOG*, Figure 2E) were not significantly different following birth; and, *OLIG2* (Figure 2F), which represents expression of the entire oligodendrocyte lineage, was also not significantly affected by birth. Importantly, genes involved in the transport and translation of *MBP* mRNA were differentially expressed following birth. The gene responsible for cytoplasmic transport of *MBP* mRNA (*HNRNPA2B1*, Figure 2G) was significantly decreased in both sexes following birth (males $p = 0.0005$, females $p < 0.0001$), and in females the gene responsible for *MBP* mRNA anchoring at the site of translation (*KIF1B*, Figure 2H) was also decreased after birth ($p = 0.0338$). However, the gene involved in translation of *MBP* mRNA (*PCBP1*, Figure 2I) was significantly increased in both sexes following birth (males $p = 0.0488$, females $p = 0.0321$). Means and SEM are available in the Supplementary Text.

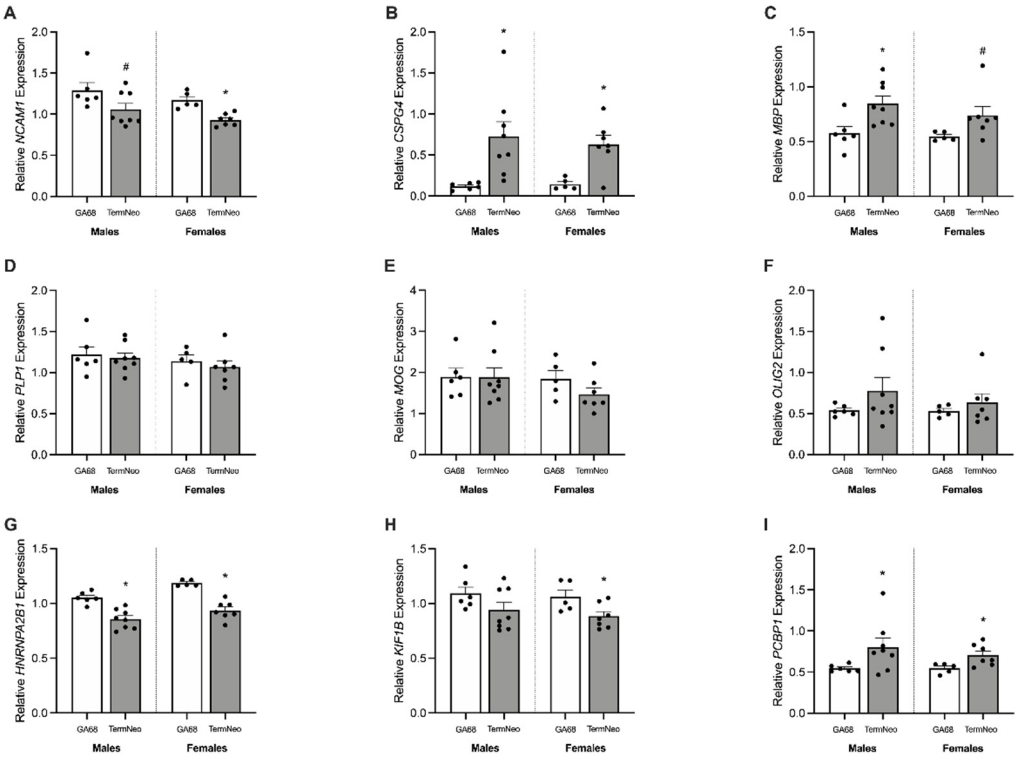

Figure 2. Relative mRNA expression for oligodendrocyte lineage and MBP translation markers in the hippocampus of fetal GA68 (white; males $n = 6$, females $n = 5$) and term neonates (grey; males $n = 8$, females $n = 7$). (**A**) *NCAM1*, (**B**) *CSPG4*, (**C**) *MBP*, (**D**) *PLP1*, (**E**) *MOG*, (**F**) *OLIG2*, (**G**) *HNRNPA2B1*, (**H**) *KIF1B*, and (**I**) *PCBP1*. Data presented as means ± SEM with * indicating significance at $p < 0.05$, and # representing a non-significant trend.

In addition to oligodendrocyte markers, the relative mRNA expression of neuronal markers in the hippocampus was also quantified (Figure 3). The expression of GABAergic interneurons was differentially affected by birth with a reduction in *CALB1* (calbindin, Fig-

ure 3A) expression in term male neonates compared to fetal ($p = 0.0031$), and the expression of *PVALB* (parvalbumin, Figure 3B) and *SST* (somatostatin, Figure 3C) increased in neonates compared to fetuses (*PVALB*: males $p = 0.0096$, females $p = 0.0056$; *SST*: females $p = 0.0040$); however, this didn't reach significance for *SST* in males ($p = 0.0524$). Similarly, expression of *RBFOX3* (neurons; Figure 3D) was also significantly increased in female neonates ($p = 0.0199$) but did not reach significance in males ($p = 0.0699$). As expected, following on from these results, the expression of neuron assembly (*INA*, Figure 3E) and synaptic activity (*SYP*, Figure 3F) genes was also significantly increased following birth in both sexes (*INA*: males $p = 0.0017$, females $p = 0.0216$; *SYP*: males $p = 0.0067$, females $p = 0.0064$). Interestingly, the expression of calpains (*CAPN1*, *CAPN2*, and *CAPNS1*; Figure 3G–I), which are responsible for cell proliferation, adhesion, and motility during neurogenesis and remodeling, was also significantly increased in term neonates compared to fetal (*CAPN1*: males $p = 0.0002$, females $p < 0.0001$; *CAPN2*: males $p < 0.0001$, females $p = 0.0004$; and *CAPNS1*: females $p = 0.0276$). Means and SEM are available in the Supplementary Text.

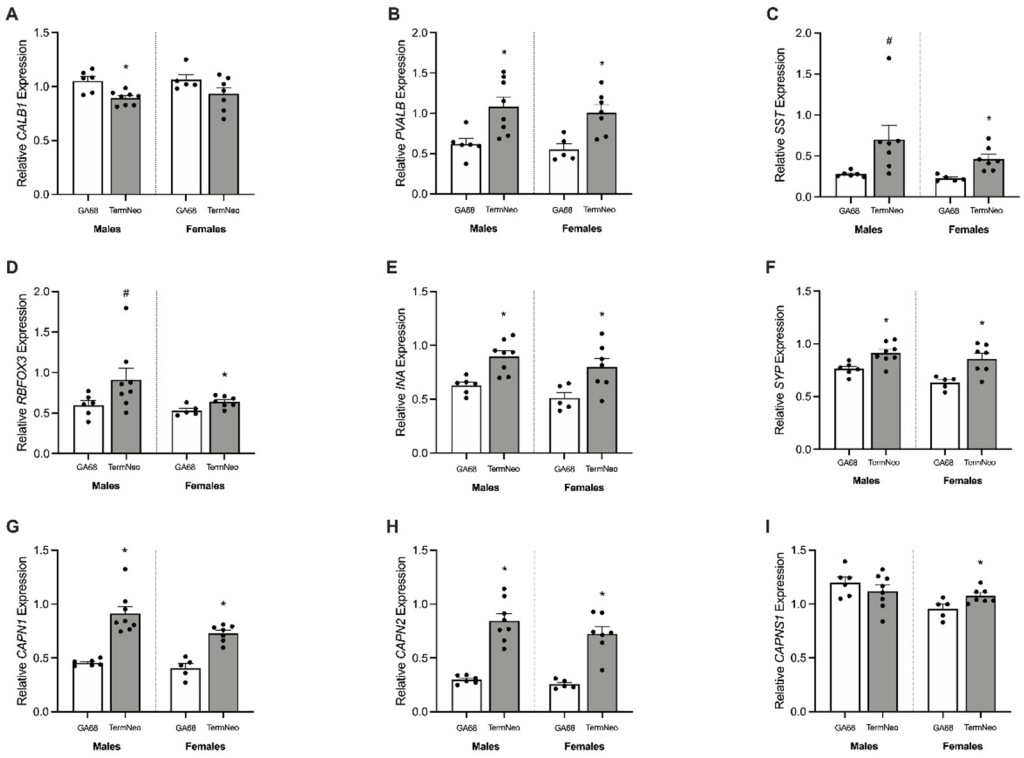

Figure 3. Relative mRNA expression for neuron and neuronal growth markers in the hippocampus of fetal GA68 (white; males $n = 6$, females $n = 5$) and term neonates (grey; males $n = 8$, females $n = 7$). (**A**) *CALB1*, (**B**) *PVALB*, (**C**) *SST*, (**D**) *RBFOX3*, (**E**) *INA*, (**F**) *SYP*, (**G**) *CAPN1*, (**H**) *CAPN2*, and (**I**) *CAPNS1*. Data presented as means ± SEM with * indicating significance at $p < 0.05$, and # representing a non-significant trend.

3.4. Expression of GABAergic Synthetic Enzymes and Transporters

The relative mRNA expression of genes responsible for GABA synthesis and transport were significantly altered following birth. The relative expression of synthetic enzyme *GAD1(67)* (Figure 4A) was significantly increased in male term neonates ($p = 0.0003$), while the expression of *GAD2* (Figure 4B) increased in term females ($p = 0.0312$) but did not reach significance in males ($p = 0.0759$). The expression of *ABAT* (Figure 4C), the gene responsible for GABA breakdown, was not significantly different between fetuses and term neonates of either sex. Expression of the gene responsible for packaging of GABA into synaptic vesicles was significantly increased following birth (*SLC32A1*; vGAT) (Figure 4D, males $p = 0.0469$, females $p = 0.0475$) in addition to the expression of synaptic reuptake transporters (*SLC6A1*;

GAT1 and *SLC6A11*; GAT3) (Figure 4E,F), which were upregulated in males only ($p = 0.0020$ and $p = 0.0155$, respectively). Means and SEM are available in the Supplementary Text.

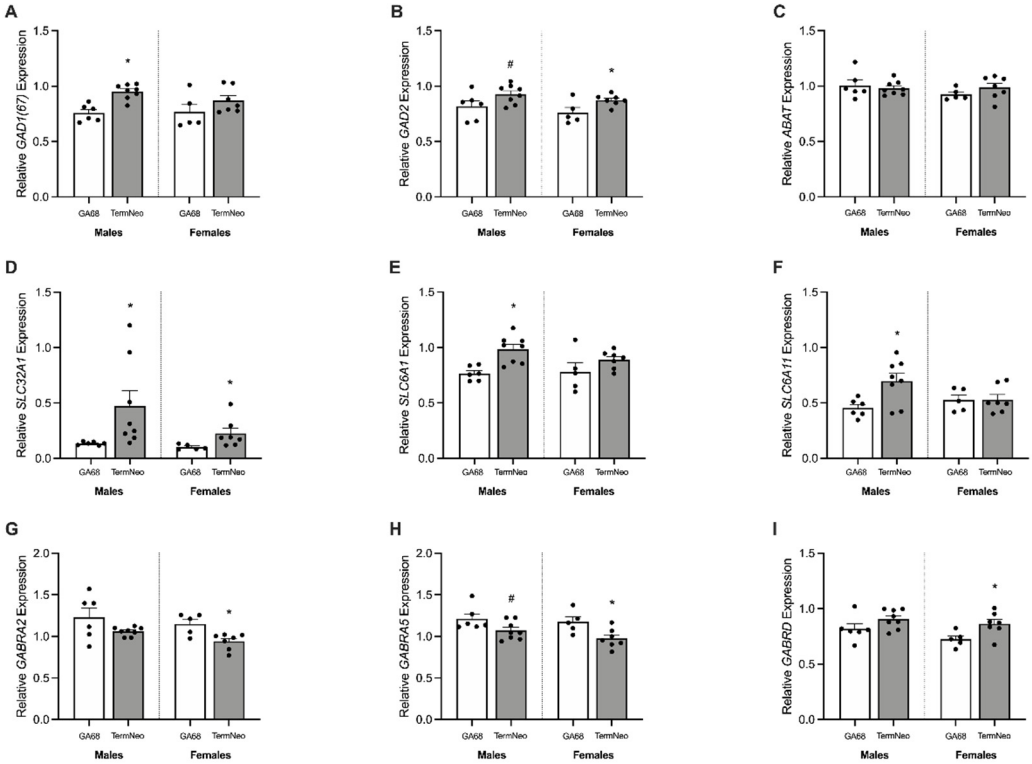

Figure 4. Relative mRNA expression for GABA synthesis, breakdown, transport, and receptor markers in the hippocampus of fetal GA68 (white; males $n = 6$, females $n = 5$) and term neonates (grey; males $n = 8$, females $n = 7$). (**A**) *GAD1(67)*, (**B**) *GAD2*, (**C**) *ABAT*, (**D**) *SLC32A1*, (**E**) *SLC6A1*, (**F**) *SLC6A11*, (**G**) *GABRA2*, (**H**) *GABRA5*, and (**I**) *GABRD*. Data presented as means ± SEM with * indicating significance at $p < 0.05$, and # representing a non-significant trend.

3.5. $GABA_A$ Receptor Subunit Expression

Neurosteroid-sensitive extrasynaptic $GABA_A$ receptors were also differentially affected, with a significant reduction in *GABRA2* (Figure 4G) and *GABRA5* (Figure 4H) mRNA expression in term females ($p = 0.0089$ and $p = 0.0204$, respectively) but with an increase in *GABRD* mRNA (Figure 4I, $p = 0.0283$); *GABRA5* expression also appeared to be reduced in term males but this did not reach significance ($p = 0.0605$). Means and SEM are available in the Supplementary Text.

3.6. Changes to the Glutamatergic Pathway

The expression of genes that regulate hippocampal glutamatergic pathways were significantly altered following birth. The gene responsible for glutamate synthesis *GLS1* (glutaminase, Figure 5A) was significantly reduced in term neonates of both sexes compared to fetal expression (males $p = 0.0205$ and females $p = 0.0212$). However, the expression of genes responsible for glutamate synaptic release (*SLC17A8*; vGLUT3) (Figure 5B) and re-uptake from the extracellular space (*SLC1A2*; EAAT2) (Figure 5C) were significantly increased in term neonates compared to fetuses of both sexes (*SLC17A8*: males $p = 0.0033$, females $p = 0.0005$; and *SLC1A2*: males $p < 0.0001$, females $p = 0.0058$). Along with this increase in glutamate transporters, the genes responsible for glutamate receptors (*GRIA2*, *GRIN1*, *GRIN2C*, *GRIN3A*, and *GRM1*; Figure 5D–H) involved in excitatory synaptic transmission were also significantly increased in both sexes following birth (*GRIA2*: males $p < 0.0001$, females $p < 0.0001$; *GRIN1*: $p = 0.0113$, females $p = 0.0211$; *GRIN2C*: males $p = 0.0003$, females $p = 0.0018$; *GRIN3A*: males $p = 0.0074$, females $p = 0.0112$; and *GRM1*: males $p = 0.0034$,

females $p = 0.0121$). Importantly, a key gene involved in memory formation and learning through its interactions with glutamate receptors (*DLG4*, postsynaptic density protein) is also significantly increased in term neonates of both sexes (Figure 5I, males $p = 0.0004$ and females $p = 0.0092$). Means and SEM are available in the Supplementary Text.

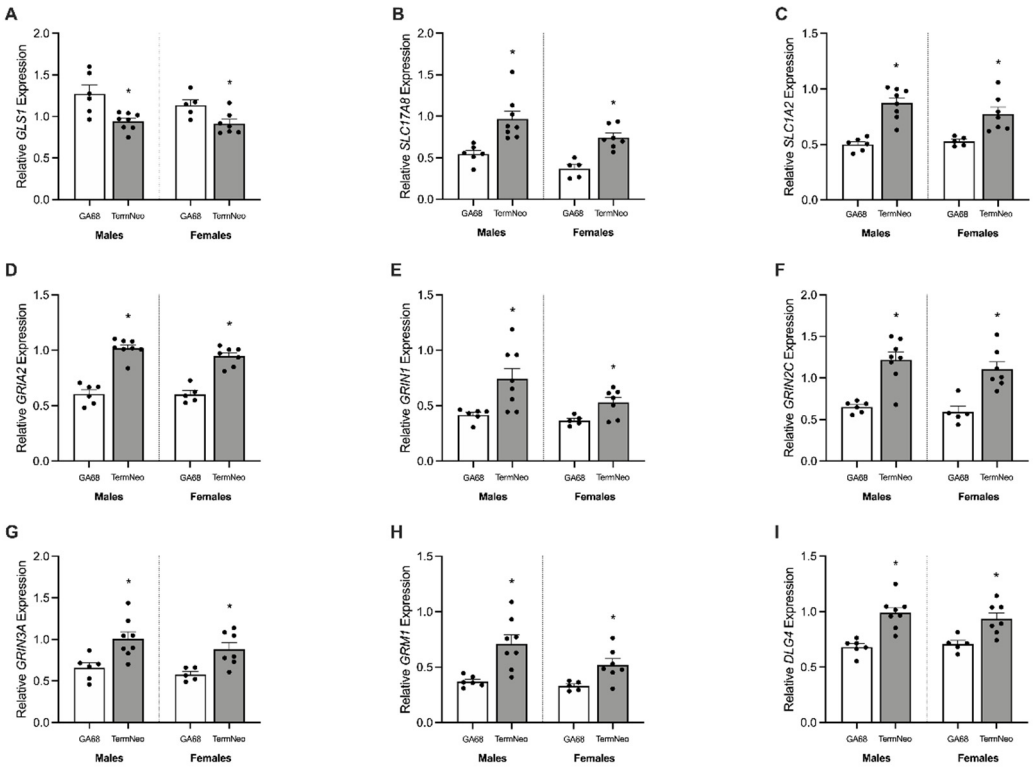

Figure 5. Relative mRNA expression for glutamate synthesis, transport, and receptor markers in the hippocampus of fetal GA68 (white; males $n = 6$, females $n = 5$) and term neonates (grey; males $n = 8$, females $n = 7$). (**A**) *GLS1*, (**B**) *SLC17A8*, (**C**) *SLC1A2*, (**D**) *GRIA2*, (**E**) *GRIN1*, (**F**) *GRIN2C*, (**G**) *GRIN3A*, (**H**) *GRM1*, and (**I**) *DLG4*. Data presented as means ± SEM with * indicating significance at $p < 0.05$.

3.7. Expression of Steroidogenic Enzymes, Transporters, and Receptors

Genes controlling the production of the neurosteroid allopregnanolone were largely unchanged in term neonates, apart from the translocator protein (*TSPO*, Figure 6A) which is responsible for bringing cholesterol into the cell for steroidogenesis. The expression of *TSPO* mRNA was significantly increased in term neonates (males $p = 0.0123$, females $p = 0.0215$), whilst the expression of *STAR* (Figure 6B, responsible for cholesterol to pregnenolone conversion) and *SRD5A1* (Figure 6C, rate-limiting enzyme in allopregnanolone and androgen production) was not significantly different between fetuses and neonates for either sex. Expression of glucocorticoid (*NR3C1*, Figure 6D) and mineralocorticoid receptors (*NR3C2*, Figure 6E) were also largely unaffected, with an apparent decrease in *NR3C1* expression in term neonates not reaching significance (males $p = 0.0740$ and females $p = 0.0703$). Lastly, the mRNA expression of *DNMT1* (DNA methyltransferase 1, Figure 6F), which is responsible for the transfer of methyl groups and may ultimately result in transcriptional silencing, was significantly increased following birth (males $p = 0.0114$ and females $p = 0.0249$). Means and SEM are available in the Supplementary Text.

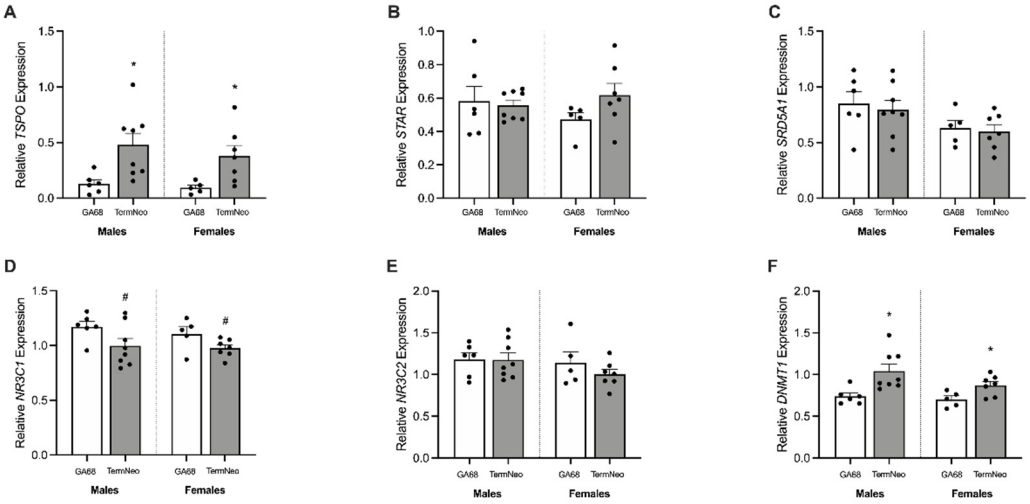

Figure 6. Relative mRNA expression for steroid synthesis and receptor markers, and DNA methyltransferase enzyme in the hippocampus of fetal GA68 (white; males $n = 6$, females $n = 5$) and term neonates (grey; males $n = 8$, females $n = 7$). (**A**) *TSPO*, (**B**) *STAR*, (**C**) *SRD5A1*, (**D**) *NR3C1*, (**E**) *NR3C2*, and (**F**) *DNMT1*. Data presented as means ± SEM with * indicating significance at $p < 0.05$, and # representing a non-significant trend.

4. Discussion

This study aimed to determine the key changes in hippocampal development that occur following the transition from in utero to ex utero life. The studies were performed in the developmentally relevant guinea pig, which has a relatively long gestation and a mature inhibitory pathway by the time of birth [22]. Neurosteroid-GABAergic interactions at this time are protective and suppress excitability, and they have been identified as pathways that may be targeted to improve outcomes following perinatal compromise [1,24,25]. The major findings, at the protein level, were that there are no differences in mature myelin coverage in the CA1 region of the hippocampus itself, but there was a reduction in the overlying subcortical white matter. This may represent a fine tuning of synaptic connections upon exposure to ex utero life and a shift from inhibitory to excitatory environment. In both the hippocampus and subcortical white matter there is an apparent increase in neuronal nuclei coverage, which again may be due to the shift from an inhibitory 'myelin promoting' environment in utero to an excitatory cell growth environment ex utero.

The cells of the oligodendrocyte lineage were identifiable by specific markers, and the effects on cell numbers at each stage were evaluated. Rapid and extensive myelination in late gestation makes this process vulnerable to changes to the in utero environment, and it highlights the devastating effect that preterm birth and other perinatal compromises during this time can have on myelination [15,21,26]. In the present study, the mRNA expression of oligodendrocyte pre-progenitor cells (*NCAM1*) was reduced following birth which is to be expected as these cells become committed to the oligodendrocyte lineage [13,27]. The finding of increases in transcription of immature (*CSPG4*) and mature (*MBP*) oligodendrocyte markers suggests an increase in these cell types following birth. This may be in response to a burst in new synaptic connections being required for ex utero functions; but, based on the protein data for MBP, this is yet to be translated within the first 24 h of ex utero life. The process of *MBP* mRNA to protein translation is complex with mRNA transcription and trafficking to the site of required translation occurring prior to translation, requiring additional key proteins [12,27]. In the present study, we observed a reduction in the gene responsible for the cytoplasmic transport of *MBP* mRNA (*HNRNPA2B1*) and the gene responsible for mRNA anchoring at the site of translation (*KIF1B*). Interestingly, the gene required for MBP translation to occur (*PCBP1*) increased, which ultimately means that whilst *MBP* mRNA and the regulator of its translation are increased the transport mechanisms between these two stages is limiting this process. It is unclear why this process is rate limiting, but it may

be in part due to the need for appropriate myelination of connections based on functions rather than widespread myelination.

In line with an increase in neuronal nuclei protein after birth, there was also an increase in mRNA for neurons (*RBFOX3*) as well as genes required for their assembly (*INA*) and for calpains (*CAPN1*, *CAPN2*, *CAPNS1*), which facilitate neurogenesis and adhesion during periods of remodeling [28]. To further characterize this neuronal population, we measured mRNA markers of GABAergic interneurons and found that overall, these were also increased following birth (*PVALB* and *SST*). Interestingly, GABAergic interneurons are known to be myelinated, supporting the contention that new synaptic connections must form prior to their myelination [29,30]. The present findings further indicate that there is an increase in new synaptic connections, with a marked increase in the major marker of neurons involved with synaptic transmission (*SYP*). There are very marked differences in the environment of the fetus compared to the neonate, including the need for processing external sensory information, and for providing protection for the still developing brain without maternal and placental support. The need for increased protection from excessive excitation after birth may drive the observed increase in the inhibitory GABAergic interneuron population. The appropriate balance of the inhibitory versus excitatory activity is essential in the late fetal and early neonatal brain, with key mRNA markers of these two pathways also examined. The correct balance of inhibitory and excitatory action is essential for proper neurodevelopment and differs depending on the period of gestation [31–33]. In the present study, there were stark changes in the mRNA expression of key components of these pathways following birth. Importantly, the synthesis of GABA from glutamate may be increased as genes responsible for its production [*GAD1(67)* and *GAD2*] rise, with no opposing decrease in the enzyme responsible for breakdown (*ABAT*). These observations suggest compensatory changes for the loss of allopregnanolone after birth. Similarly, key transporters of GABA were also increased, allowing it to be transported into the synaptic cleft (vGAT), and for unused synaptic GABA to be recycled back into the presynaptic neuron or surrounding glial cells for later use (GAT1 and GAT3). Interestingly, whilst the mRNA profile of the term neonatal hippocampus suggests an increase in production and cycling of GABA, the postsynaptic sites of action are largely unaffected. In females, there was a reduction in the *GABRA2* and *GABRA5* subunits, and in males there was an increase in the *GABRD* subunit following birth, highlighting sex differences in developmental profiles in regard to $GABA_A$ receptor subunit composition.

There were also a number of changes following birth in components of the glutamatergic excitatory system albeit in the opposite direction to those seen for the GABAergic system. The observed decreases in the gene responsible for glutamate synthesis (*GLS1*), which combined with the knowledge that glutamate to GABA production is increased, suggests that overall glutamate levels are reduced within the hippocampus. This may be a major step in regulating excessive excitation. The findings that the expression of the genes responsible for both glutamate export into (vGLUT3) and clearance from (EAAT2) the synaptic cleft were also increased further indicates that a reduction in glutamate levels follows birth. This clearance from the synaptic cleft is particularly important as excess glutamate within this space can readily lead to overactivation of receptors and excitotoxic damage [33,34]. However, glutamate is required for learning and memory through long term potentiation—which is particularly important following birth—suggesting expression of these genes is important in the fine tuning of these processes [35].

Overall, this study has identified numerous changes in major neurodevelopmental systems such as the oligodendrocyte lineage, neuronal assembly and populations, and GABAergic and glutamatergic pathways that occur during the rapid fetus to neonate transition at birth. These stark changes that are evident in normal fetal and neonatal populations therefore represent key adaptations required for the change in environment from in utero to ex utero. With the knowledge of major alterations in these hippocampal neurodevelopmental markers now comes the ability to identify inappropriate deficits or

increases in cases of perinatal compromise, and it may also lead to the identification of new therapeutic targets for improving postnatal brain development.

Supplementary Materials: The following supporting information can be downloaded at: https://www.mdpi.com/article/10.3390/reprodmed3020008/s1, Table S1: Area coverage percentage for MBP and NeuN in the hippocampus, Table S2: Relative mRNA expression of neurodevelopmentally-related genes in hippocampus.

Author Contributions: Conceptualization, J.C.S., R.M.D., H.K.P., M.J.B. and J.J.H.; data curation, J.C.S., R.M.D., H.K.P. and G.K.C.; funding acquisition, J.C.S., R.M.D., H.K.P., M.J.B. and J.J.H.; methodology, J.C.S., R.M.D., H.K.P., G.K.C., M.J.B. and J.J.H.; project administration, J.C.S., R.M.D., H.K.P., M.J.B. and J.J.H.; supervision, H.K.P., M.J.B. and J.J.H.; writing—original draft, J.C.S.; writing—review and editing, R.M.D., H.K.P., G.K.C., M.J.B. and J.J.H. All authors have read and agreed to the published version of the manuscript.

Funding: This research was funded by the Neurological Foundation of New Zealand (Wellington, New Zealand), the National Health and Medical Research Council (NHMRC) (grant number APP1003517) (Newcastle, Australia), and the Otago Foundation Trust (Preterm Birth Philanthropic Support) (Wellington, New Zealand). RMD was supported by a University of Otago Health Sciences Career Development Fellowship.

Institutional Review Board Statement: The animal study protocol was approved by the Institutional Review Board of the University of Otago, Wellington for studies involving animals in accordance with the National Ethics Advisory Committee of New Zealand.

Informed Consent Statement: Not applicable.

Acknowledgments: We acknowledge Ryan Sixtus, Heather Barnes, Maureen Prowse, and Taylor Wilson for their contributions to the animal work.

Conflicts of Interest: The authors declare no conflict of interest.

References

1. Hirst, J.J.; Kelleher, M.A.; Walker, D.W.; Palliser, H.K. Neuroactive steroids in pregnancy: Key regulatory and protective roles in the foetal brain. *J. Steroid Biochem. Mol. Biol.* **2014**, *139*, 144–153. [CrossRef] [PubMed]
2. Hirst, J.J.; Palliser, H.K.; Yates, D.M.; Yawno, T.; Walker, D.W. Neurosteroids in the fetus and neonate: Potential protective role in compromised pregnancies. *Neurochem Int.* **2008**, *52*, 602–610. [CrossRef] [PubMed]
3. Belelli, D.; Lambert, J.J. Neurosteroids: Endogenous regulators of the GABA(A) receptor. *Nat. Rev. Neurosci.* **2005**, *6*, 565–575. [CrossRef] [PubMed]
4. Nicol, M.B.; Hirst, J.J.; Walker, D.W. Effect of finasteride on behavioural arousal and somatosensory evoked potentials in fetal sheep. *Neurosci. Lett.* **2001**, *306*, 13–16. [CrossRef]
5. Yawno, T.; Yan, E.B.; Hirst, J.J.; Walker, D.W. Neuroactive steroids induce changes in fetal sheep behavior during normoxic and asphyxic states. *Stress* **2011**, *14*, 13–22. [CrossRef]
6. Yawno, T.; Miller, S.L.; Bennet, L.; Wong, F.; Hirst, J.J.; Fahey, M.; Walker, D.W. Ganaxolone: A New Treatment for Neonatal Seizures. *Front. Cell. Neurosci.* **2017**, *11*, 246. [CrossRef]
7. Shaw, J.C.; Dyson, R.M.; Palliser, H.K.; Gray, C.; Berry, M.J.; Hirst, J.J. Neurosteroid replacement therapy using the allopregnanolone-analogue ganaxolone following preterm birth in male guinea pigs. *Pediatr. Res.* **2019**, *85*, 86–96. [CrossRef]
8. Yawno, T.; Aridas, J.; Sutherland, A.; Malhotra, A.; Bennet, L.; Jenkin, G.; Walker, D.; Miller, S.; Fahey, M. The effects of ganaxolone in hypoxic ischaemic term lambs. In Proceedings of the 10th Hershey Conference on Developmental Brain Injury, Ecquevilly, France, 8–11 June 2016.
9. Shaw, J.C.; Palliser, H.K.; Dyson, R.M.; Hirst, J.J.; Berry, M.J. Long-term effects of preterm birth on behavior and neurosteroid sensitivity in the guinea pig. *Pediatr Res.* **2016**, *80*, 275–283. [CrossRef]
10. Shaw, J.C.; Palliser, H.K.; Dyson, R.M.; Berry, M.J.; Hirst, J.J. Disruptions to the cerebellar GABAergic system in juvenile guinea pigs following preterm birth. *Int. J. Dev. Neurosci.* **2018**, *65*, 1–10. [CrossRef]
11. Palliser, H.K.; Kelleher, M.A.; Tolcos, M.; Walker, D.W.; Hirst, J.J. Effect of postnatal progesterone therapy following preterm birth on neurosteroid concentrations and cerebellar myelination in guinea pigs. *J. Dev. Orig. Health Dis.* **2015**, *6*, 350–361. [CrossRef]
12. Crombie, G.K.; Palliser, H.K.; Shaw, J.C.; Hodgson, D.M.; Walker, D.W.; Hirst, J.J. Effects of prenatal stress on behavioural and neurodevelopmental outcomes are altered by maternal separation in the neonatal period. *Psychoneuroendocrinology* **2021**, *124*, 105060. [CrossRef] [PubMed]

13. van Tilborg, E.; de Theije, C.G.M.; van Hal, M.; Wagenaar, N.; de Vries, L.S.; Benders, M.J.; Rowitch, D.H.; Nijboer, C.H. Origin and dynamics of oligodendrocytes in the developing brain: Implications for perinatal white matter injury. *Glia* **2018**, *66*, 221–238. [CrossRef] [PubMed]
14. McLaurin, J.A.; Yong, V.W. Oligodendrocytes and myelin. *Neurol. Clin.* **1995**, *13*, 23–49. [CrossRef]
15. Volpe, J.J.; Kinney, H.C.; Jensen, F.E.; Rosenberg, P.A. The developing oligodendrocyte: Key cellular target in brain injury in the premature infant. *Int J. Dev. Neurosci.* **2011**, *29*, 423–440. [CrossRef]
16. Alexandrou, G.; Martensson, G.; Skiold, B.; Blennow, M.; Aden, U.; Vollmer, B. White matter microstructure is influenced by extremely preterm birth and neonatal respiratory factors. *Acta Paediatr.* **2014**, *103*, 48–56. [CrossRef]
17. Rutherford, M.A.; Supramaniam, V.; Ederies, A.; Chew, A.; Bassi, L.; Groppo, M.; Anjari, M.; Counsell, S.; Ramenghi, L.A. Magnetic resonance imaging of white matter diseases of prematurity. *Neuroradiology* **2010**, *52*, 505–521. [CrossRef]
18. Kelleher, M.; Hirst, J.J.; Palliser, H.K. Changes in neuroactive steroid concentrations after preterm delivery in the guinea pig. *Reprod. Sci.* **2013**, *20*, 1365–1375. [CrossRef]
19. Yawno, T.; Hirst, J.J.; Castillo-Melendez, M.; Walker, D.W. Role of neurosteroids in regulating cell death and proliferation in the late gestation fetal brain. *Neuroscience* **2009**, *163*, 838–847. [CrossRef]
20. Back, S.A. White matter injury in the preterm infant: Pathology and mechanisms. *Acta Neuropathol.* **2017**, *134*, 331–349. [CrossRef]
21. Back, S.A.; Han, B.H.; Luo, N.L.; Chricton, C.A.; Xanthoudakis, S.; Tam, J.; Arvin, K.L.; Holtzman, D.M. Selective vulnerability of late oligodendrocyte progenitors to hypoxia–ischemia. *J. Neurosci.* **2002**, *22*, 455–463. [CrossRef]
22. Morrison, J.L.; Botting, K.J.; Darby, J.R.T.; David, A.L.; Dyson, R.M.; Gatford, K.L.; Gray, C.; Herrera, E.A.; Hirst, J.J.; Kim, B.; et al. Guinea pig models for translation of the developmental origins of health and disease hypothesis into the clinic. *J. Physiol.* **2018**, *596*, 5535–5569. [CrossRef] [PubMed]
23. Berry, M.; Gray, C.; Wright, K.; Dyson, R.; Wright, I. Premature guinea pigs: A new paradigm to investigate the late-effects of preterm birth. *J. Dev. Orig. Health Dis.* **2015**, *6*, 143–148. [CrossRef] [PubMed]
24. Nicol, M.; Hirst, J.; Walker, D. Effect of pregnane steroids on electrocortical activity and somatosensory evoked potentials in fetal sheep. *Neurosci. Lett.* **1998**, *253*, 111–114. [CrossRef]
25. Belelli, D.; Herd, M.B.; Mitchell, E.A.; Peden, D.R.; Vardy, A.W.; Gentet, L.; Lambert, J.J. Neuroactive steroids and inhibitory neurotransmission: Mechanisms of action and physiological relevance. *Neuroscience* **2006**, *138*, 821–829. [CrossRef] [PubMed]
26. Bennett, G.A.; Palliser, H.K.; Shaw, J.C.; Palazzi, K.L.; Walker, D.W.; Hirst, J.J. Maternal stress in pregnancy affects myelination and neurosteroid regulatory pathways in the guinea pig cerebellum. *Stress* **2017**, *20*, 580–588. [CrossRef] [PubMed]
27. Bradl, M.; Lassmann, H. Oligodendrocytes: Biology and pathology. *Acta Neuropathol.* **2010**, *119*, 37–53. [CrossRef]
28. Metwally, E.; Zhao, G.; Zhang, Y.Q. The calcium-dependent protease calpain in neuronal remodeling and neurodegeneration. *Trends Neurosci.* **2021**, *44*, 741–752. [CrossRef]
29. Boulanger, J.J.; Messier, C. Oligodendrocyte progenitor cells are paired with GABA neurons in the mouse dorsal cortex: Unbiased stereological analysis. *Neuroscience* **2017**, *362*, 127–140. [CrossRef]
30. Micheva, K.D.; Chang, E.F.; Nana, A.L.; Seeley, W.W.; Ting, J.T.; Cobbs, C.; Lein, E.; Smith, S.J.; Weinberg, R.J.; Madison, D.V. Distinctive Structural and Molecular Features of Myelinated Inhibitory Axons in Human Neocortex. *eNeuro* **2018**, *5*. [CrossRef]
31. Ben-Ari, Y. Excitatory actions of GABA during development: The nature of the nurture. *Nat. Rev. Neurosci.* **2002**, *3*, 728–739. [CrossRef]
32. Coleman, H.; Hirst, J.J.; Parkington, H.C. The GABAA excitatory-to-inhibitory switch in the hippocampus of perinatal guinea-pigs. In Proceedings of the 40th Annual Meeting Fetal and Neonatal Physiological Society, Peurto Varas, Chile, 1–4 September 2014.
33. Follett, P.L.; Deng, W.; Dai, W.; Talos, D.M.; Massillon, L.J.; Rosenberg, P.A.; Volpe, J.J.; Jensen, F.E. Glutamate receptor-mediated oligodendrocyte toxicity in periventricular leukomalacia: A protective role for topiramate. *J. Neurosci.* **2004**, *24*, 4412–4420. [CrossRef] [PubMed]
34. Fu, Y.; Sun, W.; Shi, Y.; Shi, R.; Cheng, J.X. Glutamate excitotoxicity inflicts paranodal myelin splitting and retraction. *PLoS ONE* **2009**, *4*, e6705. [CrossRef] [PubMed]
35. Barnes, J.R.; Mukherjee, B.; Rogers, B.C.; Nafar, F.; Gosse, M.; Parsons, M.P. The Relationship Between Glutamate Dynamics and Activity-Dependent Synaptic Plasticity. *J. Neurosci.* **2020**, *40*, 2793–2807. [CrossRef] [PubMed]